

ADVANCES IN THERMAL INSULATION

PROCEEDINGS OF THE EURO THERM SEMINAR N° 44

18-20 October 95 Espinho - Portugal

O R G A N I Z I N G C O M M I T T E E

Prof. Albino Reis
Lusíada University
Portugal

Prof. C.J. Hoogendoorn
Delft University of Technology
Holland

Prof. G.P. Hammond
University of Bath
United Kingdom

Edited by

ECEMEI
Rua Gago Coutinho, 185 - 187
4435 Rio Tinto - Portugal

Evacuatable Guarded Hot Plate for Thermal Conductivity Measurements between -200°C and 800°C

U. Heinemann, J. Hetfleisch, R. Caps, J. Kuhn, J. Fricke,
Bavarian Center for Applied Energy Research (ZAE Bayern),
Am Hubland, D-97074 Würzburg, Germany

Abstract

For the characterization and optimization of insulation materials and systems, especially for evacuated super insulations a hot plate device has been developed which can be operated under stationary conditions at mean temperatures between -200°C and 800°C, internal gas pressures between 10^{-5} mbar and 1000 mbar and external pressure loads of up to 4 bar. Circularly shaped samples with a diameter of 200 mm and thicknesses from 1 to 28 mm can be investigated. Emissivities of the plates from 0.04 to 0.8 may be established. A special correction procedure has been established in order to compensate residual radial heat fluxes and errors in measured temperature difference which do not depend on the temperature difference between hot and cold plates.

Keywords

hot plate apparatus, thermal conductivity, heat transfer, solid conduction, gaseous conduction, radiative transfer, coupling effects, infrared, extinction, emissivity, superinsulations

1 Introduction – Guarded Hot Plate Apparatus LOLA 3

For the characterization and for the optimization of insulation materials and insulation systems several devices to measure stationary as well as transient heat transfer have been built in our institute [1],[2],[3],[4],[5]. Aims of the investigations are to measure total heat transfer and especially to analyse the different heat transfer mechanisms [6]. Conduction via the solid skeleton, especially in porous materials [7],[8], gaseous conduction [9],[10] and radiative heat transfer [11],[12] as well as coupling effects [9],[8] can be quantified by variation of temperature, internal gas pressure, kind of gas, external pressure load, sample thickness or surface emissivity of the adjacent plates. Theoretical predictions for a broad field of parameters then are possible.

The evacuatable guarded hot plate apparatus LOLA 3 described in this report is most versatile: it can be operated at mean temperatures between -200°C and 800°C, internal gas pressures between 10^{-5} mbar and 1000 mbar and external pressure loads of up to 4 bar for circular shaped samples with a diameter of 200 mm and thicknesses from 1 to 28 mm. Different emissivities ε of the boundaries may be established, from $\varepsilon = 0.8$ for the uncovered plates down to $\varepsilon = 0.04$ if Aluminium foils are inserted between specimens and plates.

The errors to be expected in hot plate measurements have been described in detail by Bode [13]. A newly developed correction method allows to improve the measurement accuracy considerably [14].

2 Measuring Principle

A guarded circular metal plate acts as hot plate. It is temperature controlled by electrical heating and is sandwiched between two identical test samples, which are in close contact with two heat sinks. The guarded hot plate and the heat sinks are kept at constant temperatures. The electrical power fed into the hot plate is converted into a heat flux which is symmetrically transmitted through both samples and is absorbed by the heat sinks. In order to establish a one-dimensional heat flux the hot plate consists of a central plate surrounded by two guard rings, all three kept at the same temperature.

Steady state is achieved when all temperatures and heat fluxes have become stationary. Then the thermal conductivity λ of the sample can be calculated according to

$$\lambda = \frac{P_{el}D}{2A\Delta T} \quad , \quad (1)$$

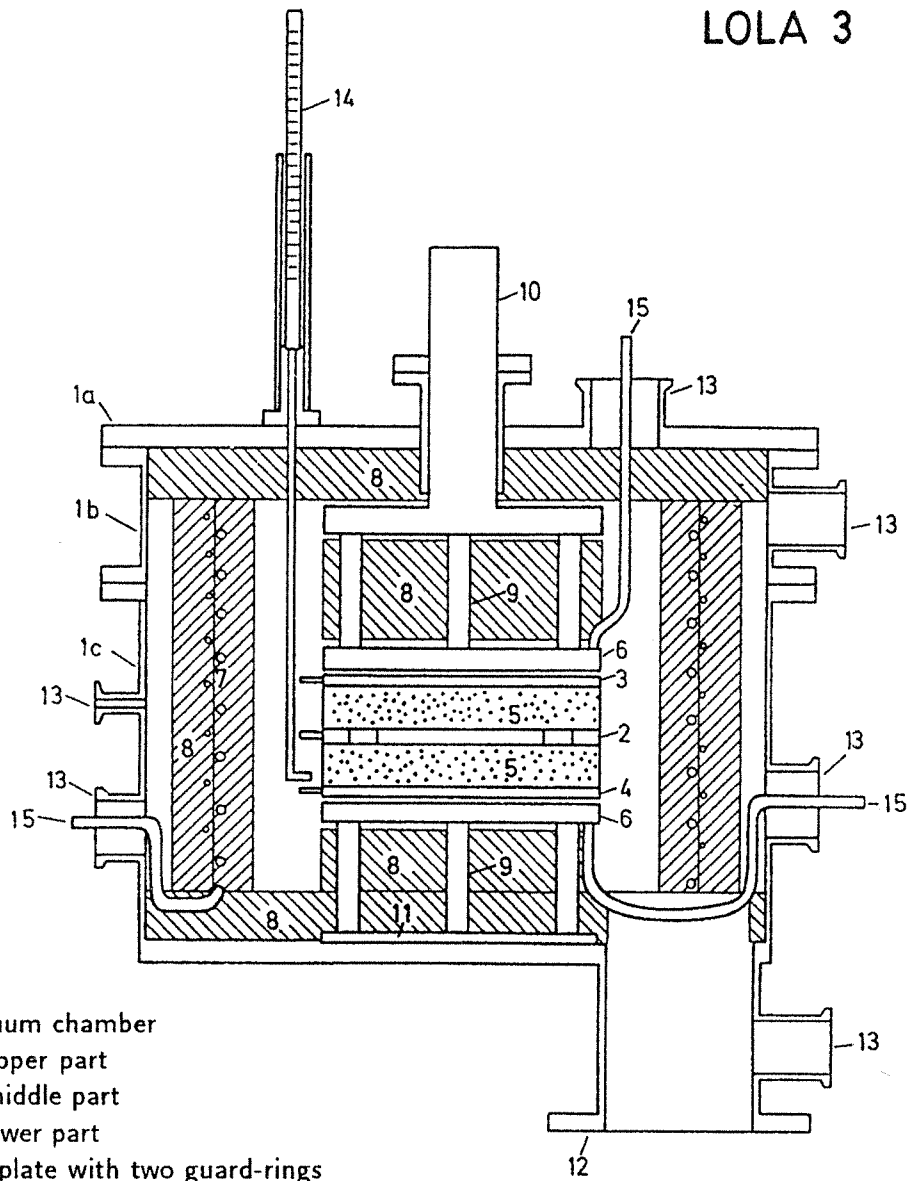
where P_{el} is the electrical power fed into the central plate in order to keep the temperature difference ΔT between the hot and cold sides of the samples constant, A is the area of the central hot plate and D the sample thickness.

3 Description of Apparatus LOLA 3

The components of apparatus LOLA 3 are (see also fig. 1):

- a cylindrical vacuum chamber made from stainless steel, with a diameter of 450 mm, a height of 340 mm (1a, 1b, 1c) with various flanches (12,13);
- one hot and two cold plates (2, 3, 4) made from a tungsten alloy (W94Cu4Ni2), with a diameter of 200 mm where the central heating section of the hot plate with a diameter of 120 mm is surrounded by two guard rings (outer diameter 160 mm and 200 mm respectively) (2);
- an inner thermal insulation of the vacuum chamber (8) using SiO₂-fiber insulation with an auxiliary heating or cooling facility mounted on Nickel sheets (7) in the center;
- 2 cooling units (6) made of Inconel 600 with fluid pipes (15) to be driven with pressurized air, cooling fluid (water or liquid nitrogen) or without any medium; the cooling units are separated from the cold plates by 1 mm calcium silicate sheets as thermal resistances;
- 10 ceramic supports, diameter 15 mm, height 100 mm (9) and high temperature insulation (8);
- 3 sensors for measurement of sample thickness (14);
- a movable, vacuum tight piston (10) to transduce a mechanical load from outside onto the specimens;
- vacuum pump system with oil diffusion pump and rotary slide pump;
- personal computer with printer and ECB-card;
- ECB-Bus module with 10 Digital-Analog-Converters (12 bit), security switch with watch-dog-function and an IEEE-interface;

LOLA 3



- | | | | |
|----|--------------------------------|----|----------------------|
| 1 | vacuum chamber | | |
| a. | upper part | | |
| b. | middle part | | |
| c. | lower part | | |
| 2 | hot plate with two guard-rings | | |
| 3 | upper cold plate | | |
| 4 | lower cold plate | 10 | piston |
| 5 | tested specimen | 11 | ground plate |
| 6 | heat sinks | 12 | flange for pumps |
| 7 | cylindrical guard | 13 | small flanges |
| 8 | high-temperature insulation | 14 | sensor for thickness |
| 9 | ceramic support | 15 | fluid pipes |

Figure 1: *Evacuable guarded hot plate apparatus LOLA 3.*

- a $6\frac{1}{2}$ digit multimeter;
- 8 computer controlled power supplies 1 x 7.5 W, 5 x 100 W, 1 x 225 W, 1 x 625 W;
- electrical heating in vacuum is performed with vacuum tight capsuled Philips standard Thermocoax heaters SEI 10/200 and SEI 20/800 with 'cold ends';
- precision electrical shunt $1\ \Omega$, 1 W, with very low temperature dependence (overall deviation from nominal value 0.1%) for accurate measurement of the electrical heating current for the central hot plate;
- analog multiplexers for scanning up to 32 voltage signals and up to 48 platinum resistors in 4 wire technique and reed relays for connection of voltage drop at precision shunt to the multimeter;
- 2 capacitive pressure gauges (measuring range 0–1000 Pa and 0– 10^5 Pa), an ionisation and a Pirani vacuum gauge for coarse vacuum control, all with analog output 0–10 V;
- Pt-100 platinum resistors, (type W 86 by Degussa) are used as temperature sensors; they are connected in four-wire technique with leads 0.25 mm CroNiFer 30 20, placed inside the hot plate (4 Pt-100 in the central section, 3 in the inner and 2 in the outer guard ring) or at the surfaces closest to sample in the cold plates (6 at each plate), 5 additional sensors are located on the surrounding auxiliary heating shield and its insulation.

Measurement of Pt-100 resistances is performed cyclically with the scanner and the multimeter. The temperatures are calculated by the PC using individual Pt-100 calibration data.

For the determination of the heating power of the central plate the electrical heating current I is measured by the voltage drop across the precision $1\ \Omega$ shunt. The electrical power is calculated according to $P_{el} = RI^2$, where R is the temperature dependent electrical resistance of the 'hot section' of the central heater, measured at 20°C and calculated with the temperature dependence given by the manufacturer of the Thermocoax heater wire.

4 Measuring Procedure

Temperature and voltage data are registered by the computer within one measuring cycle of about 60 s duration. For each device the mean value and the standard deviation of the temperature, measured with several sensors, is calculated. The deviations from the nominal temperatures and the changes of temperature with time are used as input for the calculation of the heating powers (proportional-integral controller implemented by the computer program). After the end of each measuring cycle the power supplies are regulated by analog signals to the new power ratings. When temperatures and electrical heating power rates are stationary for at least 1.5 h the values of the last hour are averaged and the thermal conductivity is calculated according to eq. (1).

5 Measuring Accuracy

5.1 Temperature

Temperature tolerances of Pt-100 resistances are according to DIN ICE 751 between 0.6 K and 1.3 K. Additionally all Pt-100 used are taken from the same production charge. Therefore the temperature dependence, which is influenced by the composition of the platinum material, is the same for all sensors. Individual calibration data have been measured by the manufacturer for each sensor at 0°C, for 10 sensors additionally at 100°C and for 3 sensors additionally at the melting point of aluminium (660,46°C).

This procedure yields smaller tolerances; the local variation of the sensors in the central plate is in the range 0.02 K to 0.2 K. Accuracy is checked about once a year and after measurements under extreme conditions. The temperature difference ΔT between hot and cold plates is accurate within 0.5 K for temperatures up to 300°C and 1.0 K for temperatures up to 600°C. The variation of temperature with time can be kept constant by the PI-regulation within some 10^{-3} K.

5.2 Measuring area A

The measuring area of 113 cm² is accurate within 0.5%, the change of diameter with temperature (temperature coefficient $\alpha = 5.9 \cdot 10^{-6} \text{K}^{-1}$) is included in the evaluation of the data.

5.3 Electrical power P_{el}

The heater current can be measured within 0.1%. The resistance of the heating wire is estimated to be accurate within 1%; thus the heating power has a total measurement error of about 1%.

5.4 Sample thickness

The measurement accuracy of absolute sample thickness within the apparatus is about 0.2 mm or 2% relatively for a nominal thickness of 10 mm.

5.5 Radial heat losses

The temperature difference between the central hot plate and the guard ring should be zero in order to prevent radial heat fluxes. The measuring accuracy of the temperature difference is in the range between 0.05 K and 0.5 K depending on temperature. From test measurements it is known that a change of temperature difference between central plate and first guard ring of 1 K yields a change in power P_{el} in the order of 0.1 W for the evacuated chamber and 0.3 W for the air-filled chamber. This means that radial power losses are in the range of $0.3 \text{ W/K} \cdot 0.5 \text{ K} = 0.15 \text{ W}$ in the worst case. For samples with a thermal conductivity beyond $0.1 \text{ W}/(\text{m K})$ and a thickness of 1 cm a power loss of typically 2 times 0.1 W per Kelvin temperature difference between the hot and the two cold sides is measured. For a temperature difference ΔT of 40 K the measured power will thus be above 9 W with an uncertainty due to radial losses of absolute 0.15 W or less than 2%.

6 Correction Method

From measurements at the same mean temperature but with different temperature differences ΔT across the specimens (between 2 and 40 K) radial heat losses and errors in

measured temperatures, which both are supposed to be largely independent of the chosen temperature difference, can be corrected. Fig. 2 depicts measured heat transfer coefficients k versus the inverse of temperature difference $1/\Delta T$ for properly controlled guard rings and for the system with a large radial heat loss artificially generated by running the guard rings 5 K below the central section. The linear dependence obtained for both cases confirms the assumption. Extrapolation to infinite temperature difference ($1/\Delta T \rightarrow 0$) in both cases gives the same true heat transfer coefficient. In general two measurements with different temperature differences ΔT_1 and ΔT_2 are sufficient to evaluate the true heat transfer coefficient

$$k_{\text{cor}} = \frac{k_1 \Delta T_1 - k_2 \Delta T_2}{\Delta T_1 - \Delta T_2} \quad (2)$$

or the thermal conductivity

$$\lambda_{\text{cor}} = \frac{(P_1 - P_2)D}{2A(\Delta T_1 - \Delta T_2)} \quad (3)$$

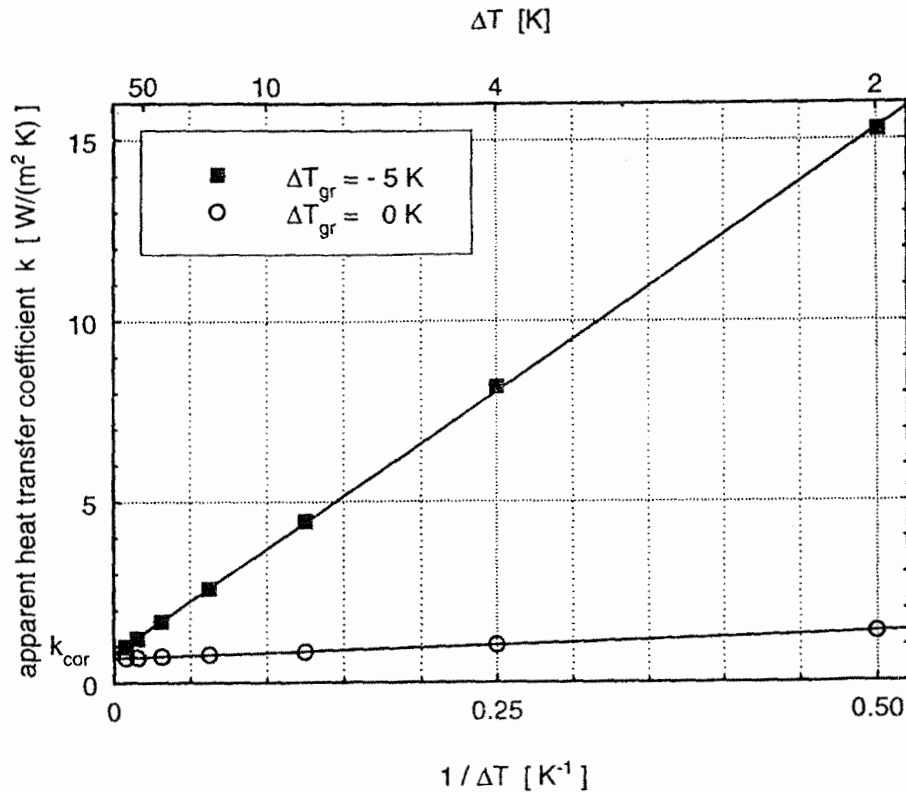


Figure 2: ΔT -correction method: measured apparent heat transfer coefficient k for different temperature differences ΔT between hot and cold plates for a measured temperature difference between central plate and guard rings $\Delta T_{\text{gr}} = 0$ K and with an enhanced artificially generated radial heat loss ($\Delta T_{\text{gr}} = -5$ K). Extrapolation $\Delta T \rightarrow \infty$ or $1/\Delta T \rightarrow 0$ gives the true k -value [14].

This correction method [14] is used especially for samples with conductivities smaller than 0.1 W/(m K) and/or for conditions where non-negligible radial losses/gains or temperature inhomogeneities are expected, for example for measurements at high temperatures.

The overall measuring uncertainty including errors of electric power, radial heat losses, sample thickness and contact resistances is about 5%.

7 Measurements

The apparatus has been used for the measurement of a wide variety of samples and insulation systems as glass fibers, ceramic fibers [7], silica aerogel monoliths, granules and powders [2],[15],[16], mineral powders [17], foams [18], foil systems [19] and peg-supported insulations [14] as well as for the analysis of the heat transfer modes and coupling effects within these materials [9],[8].

Temperature variation allows to assess the usability of the tested insulation for cryogenic, ambient or high temperatures and also to deduce the radiative conductivity. Variation of internal gas pressure gives information on the mean pore size [15] of porous insulations (fibers, powders, aerogels) and the maximum allowable background gas pressure in order not to surpass a certain total conductivity. Application of an external load on the sample is necessary to simulate the outside atmospheric pressure which a filling material of a flat evacuated panel has to sustain.

In fig. 3 the measured heat transfer coefficient k for a monolithic SiO₂-aerogel tile (density 220 kg/m³) is depicted versus the third power of the mean temperature T_{rad}^3 . This system has been investigated within the temperature range from -200°C up to 400°C without and with gas (N₂), for emissivities ε of the plates of 0.04 and 0.77.

Due to the large spectral variation of the infrared extinction (over more than 5 orders of magnitude) in SiO₂-aerogels radiation is an important or even the dominant heat transfer mechanism [16]. In these semitransparent media especially for low- ε surfaces and temperatures above 400 to 500 K, the combined radiative/conductive heat transfer is dramatically enhanced compared to a simple additive heat transfer model. Results of numerical calculations for this complex heat transfer meet the measured data very well for the whole parameter set and temperature range investigated. Deviations for the evacuated system and low ε from theory are caused by an insufficient thermal contact between samples and plates as one can conclude from a variation of gas pressure and external pressure load.

Fig. 4 gives an example for an extraordinary large coupling effect between solid and gaseous conduction (N₂). In the evacuated case the small contact areas of the spheres cause a large thermal resistance in the investigated bed of micro glass spheres (all with a diameter of 1 mm). The onset of the gaseous contribution occurs at about 1 Pa when the mean free path of the gas molecules is in the order of 1 mm. For gas pressures above 10⁴ Pa the total conductivity is 5 times larger than expected from a naive model in which conductivity of the evacuated sample λ_{vac} and gaseous conductivity of the free gas $\lambda_{gas,0}$ of 0.026 W/(m K) are superimposed.

In fig. 5 the influence of the external pressure load on the heat transfer for the evacuated system is depicted for the same sample. With an external load contact areas are enlarged, resulting in an increased heat transfer.

Acknowledgment

This work was supported by the Bavarian Ministry of Economies, Transport and Technology, Munich.

References

- [1] D. Büttner, J. Fricke, H. Reiss; *Thermal conductivity of evacuated load bearing powder and fiber insulations – Measurements with the improved 700×700 mm² variable load guarded hot plate device*; High Temp. – High Press. **17**, 333–341 (1985)

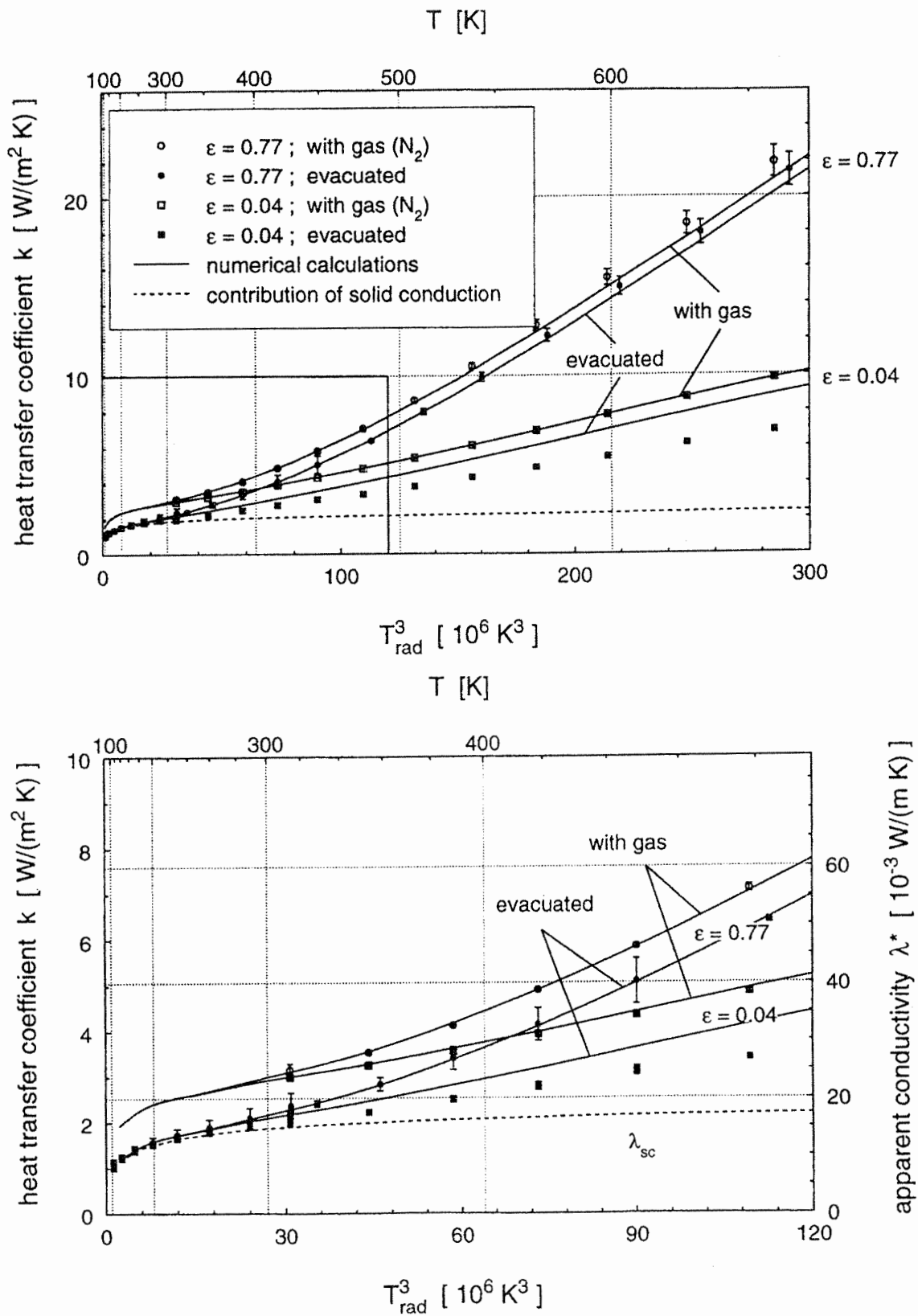


Figure 3: Measured and modelled heat transfer coefficient k versus T_{rad}^3 for an SiO_2 -aerogel tile with $\rho = 220 \text{ kg/m}^3$, thickness $d = 7.9 \text{ mm}$; parameter is the surface emissivity ϵ ; data for evacuated and non-evacuated specimens are shown [16].

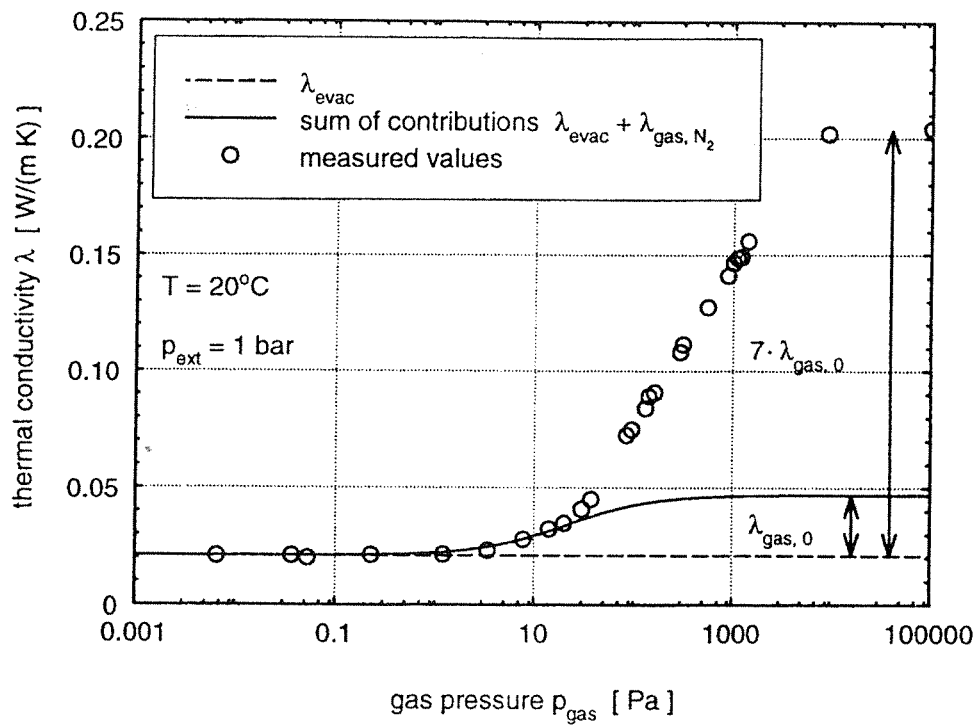


Figure 4: Influence of the gas pressure (N_2) on the thermal conductivity of a bed of glass spheres with a uniform diameter of 1 mm.

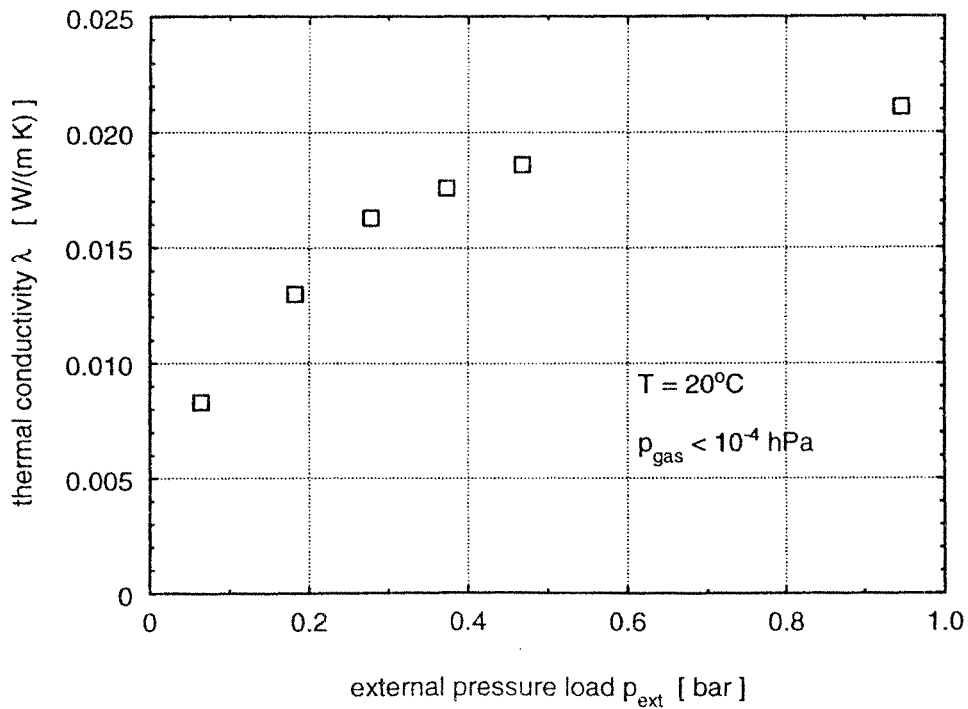


Figure 5: Influence of the external load on the thermal conductivity of a bed of glass spheres with a uniform diameter of 1 mm.

- [2] P. Scheuerpflug, R. Caps, D. Büttner, J. Fricke; *Apparent thermal conductivity of evacuated SiO₂-aerogel tiles under variation of radiative boundary conditions*; Int. J. Heat Mass Transfer **28**, 2299–2306 (1985)
- [3] R. Caps, G. Döll, J. Fricke, U. Heinemann, J. Hetfleisch; *Thermal Transport in Monolithic Silica Aerogel* in R. Vacher, J. Phalippou, T. Woigner (editors), *Proceedings of the 2nd International Symposium on Aerogels (ISA 2)*, Revue de Physique Appliquée, Colloque C4, Suppl.4, Tome 24, Les éditions des Physique, Les Ulis (1989)
- [4] T. Rettelbach, J. Säuberlich, S. Korder, J. Fricke; *Thermal conductivity of IR-opacified silica aerogel powders between 10 K and 275 K*; J. Phys. D: Appl. Phys. **28**, 581–587 (1995)
- [5] H. P. Ebert, V. Bock, O. Nilsson, J. Fricke; *The hot-wire method applied to porous materials of low thermal conductivity*; High Temp. – High Press. **25**, 391–402 (1993)
- [6] D. Büttner, J. Fricke; *Analysis of radiative and solid conduction components of the total thermal conductivity of an evacuated glass fiber insulation – Measurements with a 700×700 mm² variable load guarded hot plate device*; Proc. AIAA 85-1019, 20th Thermophys. Conf. Williamsburg (1985)
- [7] D. Büttner, G. Löffler, R. Caps, J. Fricke; *Investigation of Solid Conduction in Evacuated Load-Bearing Fibrous Insulations*; High Temp. – High Press. **18**, 537–543 (1986)
- [8] U. Heinemann; *Wärmetransport in semitransparenten nichtgrauen Medien am Beispiel von SiO₂-Aerogelen*; thesis, University of Würzburg / Germany (1993)
- [9] C. Stark, J. Fricke; *Improved Heat Transfer Models from Fibrous Insulations*; Int. J. Heat Mass Transfer **36**, 617–625 (1993)
- [10] U. Heinemann, E. Hümmer, D. Büttner, R. Caps; *Silica aerogel – a light-transmitting thermal insulator*; High Temp. – High Press. **18**, 517–526 (1986)
- [11] R. Caps, K. Baumeister, J. Fricke; *Radiative Transfer in Thermal Insulations of Low Optical Density*, High Temp. – High Press. **18**, 589–597 (1986)
- [12] R. Caps, J. Fricke, H. Reiss; *Radiative Heat Transfer in Anisotropically Scattering Fiber Insulations*; High Temp. – High Press. **17**, 303–309 (1985)
- [13] K.H. Bode; *Wärmeleitfähigkeitsmessungen mit dem Plattengerät: Einfluß der Schutzringbreite auf die Meßunsicherheit*; Int. J. Heat Mass Transfer **23**, 961–970 (1980)
- [14] J. Hetfleisch; *Wärmetransport in bereichsweise gestützten Vakuum-Superisolationen*; thesis, University of Würzburg / Germany (1995)
- [15] J. Fricke; *Materials research for the optimization of thermal insulations*; High Temp. – High Press. **25**, 379–390 (1993)
- [16] U. Heinemann, R. Caps, J. Fricke; *Radiation/Conduction Interaction on Silica Aerogels*; accepted for publication in Int. J. Heat Mass Transfer (1995).
- [17] K.G. Degen, E. Hümmer, R. Caps, J. Fricke; *Heat transfer in load-bearing diatomite powder insulations*; High Temp. – High Press. **20**, 593–598 (1988)
- [18] J. Kuhn, H.P. Ebert, M.C. Arduini-Schuster, J. Fricke; *Thermal Transport in Polystyrene and Polyurethane Foam Insulations*; Int. J. Heat Mass Transfer **35**, 1795–1801 (1992)
- [19] K.G. Degen, S. Rossetto, J. Fricke; *Heat Transfer in Evacuated Crinkled or Embossed Multilayer Foil Insulations*; J. Thermal Insulation and Building Envelopes **16**, 340 (1993)